When less is more: does more Na + -cations mean more adsorption sites for toluene in faujasites?

G C Q da Silva, Jean-Marc Simon, J. Marcos Salazar

When less is more: more Na^+-cations means more adsorption sites for toluene in faujasites?

G. C. Q. da Silva, J. M. Simon, and J. Marcos Salazar*

Laboratoire ICB UMR 6303, Université Bourgogne Franche-Comté, 21078 Dijon, France

E-mail: *jmarcos@u-bourgogne.fr

Abstract

The unique properties of zeolites makes them an interesting material to be used in separation processes. The possibility of tailoring some of their characteristics, like the Si/Al ratio, allows to optimize their synthesis for a given task. Concerning the adsorption of toluene by faujasites an understanding of the effect of cations is necessary to foster the elaboration of new materials, which can capture molecules with a high degree of selectivity and sensibility. Undoubtedly, this knowledge is relevant for a wide range of applications going from the elaboration of technologies for improving the air-quality or diagnostic procedures to prevent health risks. The studies reported here by Grand Canonical Monte Carlo elucidate the role of Na-cations in the adsorption of toluene by faujasites with different Si/Al ratios. They detail how the location of the cations inhibits or enhances the adsorption. The cations located at site II are shown to be those enhancing the adsorption of toluene in faujasites. Interestingly, cations located at site III generate a hindrance at high loading. This becomes an impediment for the organization of toluene molecules inside the faujasite.

1 Introduction

Toluene is a well known aromatic compound used as a reagent in the synthesis of different chemicals and as a solvent in many industries. Together with benzene, ethyl-benzene, and xylene, toluene composes the so-called BTEX group of volatile organic compounds (VOC's). They are related to many health risks ranging from neurological disorders to cancer. These compounds act as pollutants because of their possible influence in chemical processes that occur at the troposphere.[1,2] These issues lead to many regulations worldwide for controlling the level of toluene in different environments.[3,4] Henceforth, there is a need for developing strategies for separating or degrading toluene by adsorption or chemical conversion processes.[5] If we address the adsorption processes for capturing airborne toluene, many materials have been studied such as: activated carbon, metal-organic frameworks, clays, ionic liquids and zeolites.[5–7] Zeolites present a low production cost, they appear as a promising alternative for the adsorption of toluene. Other interesting properties of this material are their high thermal stability and the possibility of tailoring them (c.f. modification of the Si/Al ratio and the chemical nature of exchanged cations). The faujasite structure is attractive because the cage and channel diameters allow for an efficient capture of many molecules. More specifically, it was reported that the largest sphere diameter that can be included inside the pore is about 11.24 Å and of a sphere that can diffuse in the direction of each cell vector is about 7.35 Å.[8]

Molecular modeling of zeolites is interesting since it allows to study in detail the adsorption process and correlate them with the modifiable characteristics of the material. Namely, the comprehension of the effect of cations on the competing adsorption of water and toluene could be of great value for addressing an important technological challenge: the synthesis of a material able of adsorbing toluene at environments with different levels of humidity.[9–12] Moreover, toluene can be seen as a bio-marker for lung cancer.[13] Thus, designing a material capable of detecting very-low quantities (some ppb) of toluene in a humid environment, such as the human breath, would open the possibility to use such systems in diagnostical procedures.[13] Although these points are technologically relevant, it is necessary to address

first the role of cations on the adsorption of toluene. Here, we started by studying the role of Na^+ cations on the adsorption of toluene in faujasites.

While the research interest resides on improving either the sensibility or selectivity of the adsorbent, this undoubtedly requires to have a detailed picture of the cation effects on the adsorption of aromatics.

The spatial distribution of cations in a zeolite ain't random and depending on the Si/Al ratio they tend to occupy different sites (see Figure 1). Following the conventional nomenclature, faujasites with a Si/Al ratio higher than 1.8 are named NaY and NaX otherwise. The only exception is the system absent of cations, which is commonly denominated DaY as dealuminated Y zeolite.

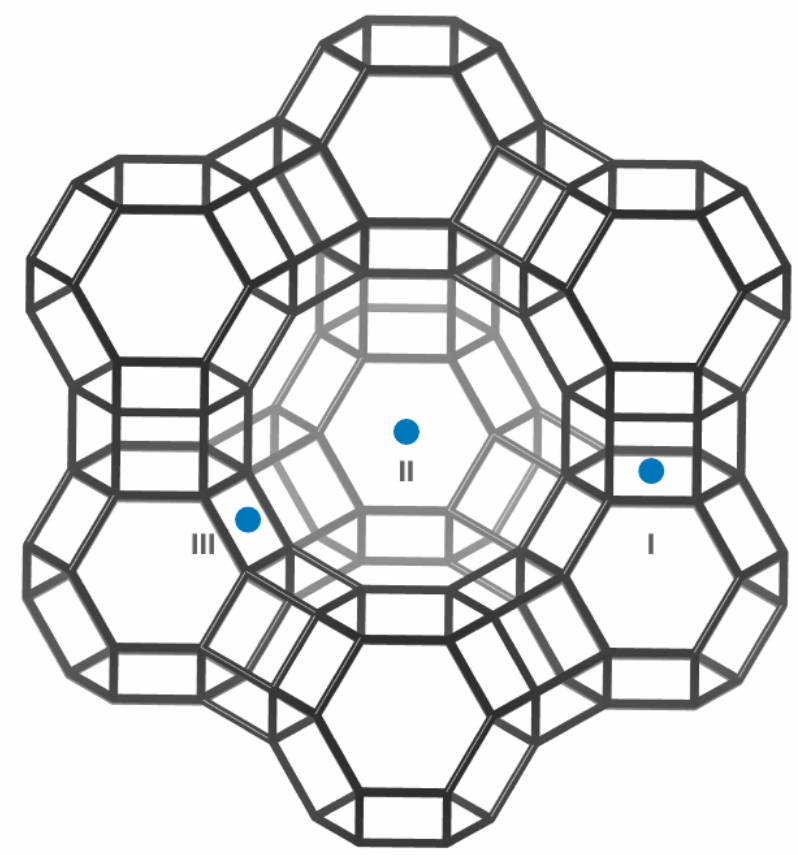

Figure 1: Location of cations at sites I, II and III for the Faujasite NaY and NaX.

In the experimental characterization of Fitch *et al.*, the authors identified preferable adsorption sites of benzene on the zeolite NaY.[14] They showed that, inside each super-cage, 4

benzene molecules are located near the cations at site II. In addition, other adsorption sites were identified near the center of the six-membered ring of the oxygen atoms (located at the windows connecting the supercages). Such results were also observed in early computational studies employing canonical Monte Carlo simulations of zeolites at a given loading.[15,16] Gonçalves *et al.* performed NMR experiments for elucidating the transport properties of adsorbed benzene molecules inside faujasites with Si/Al ratio of 2.65 (HY), 3.25 (USY) and 40 (NaY).[17] They showed that an increase in the number of cations in the zeolite reduced the mobility of the adsorbate (implying a decrease of the probability of site-hopping events). The authors argued that the lower mobility was due to the tightly interacting pairs benzene-cations at site II.

Interestingly, Auerbach and coworkers explained how the trend, mentioned in the last paragraph, is reversed if one compares NaY and NaX.[18] This last was verified by Quasi-Elastic Neutron Scattering measurements.[19] The authors argued that the hopping movements are favored in NaX by the combination of different factors. First, the presence of cations at site III decreased the stability of the pair benzene-cation of site II. Second, the adsorption occurring near the cations at site III are more favorable than the adsorption around site II. Moreover, the aromatic compound is able to interact simultaneously with cations in both sites. This would be responsible for a competition in forming interaction pairs with the adsorbate. This will ultimately enhance the mobility of the adsorbates in zeolites with higher cation quantities.[18] This non-trivial behavior, that associates the location of cations and their interactions with aromatic compounds, plays a relevant role in the adsorption capacity and selectivity of such materials. For instance, the presence of a cation in NaY makes the adsorption of toluene energetically more favorable than in high-silica zeolites (e.g., DaY). This can be explained by evoking the occurrence of specific interactions between the cations and the aromatic molecule.[13,20,21] This implies a different adsorption mechanism between the two materials. While the adsorption of benzene on NaY occurs near sites II, in DaY the sorbates are randomly distributed inside the structure. This has been reported in

Grand Canonical Monte Carlo (GCMC) simulations.[22]

However, even if the adsorption of toluene in NaX is energetically more favorable than in NaY,[23] this is not necessary followed by a higher adsorption saturation value of toluene on NaX. In fact, Daems and coworkers[23] showed that, in the NaX at high loading, there would be the formation of interacting pairs between a benzene and a sodium located either at sites II or III. Which will create a degree of steric hindrance inside the supercage. This can be associated to a change in the positions of adsorption of benzene molecules near the cage window. Given that in the NaY cations in sites III are absent, there will not be such effect. Hence, the system will show a higher adsorption capacity.[23] It is possible to argue that, since the high loading measurements are performed at the liquid phase of a mixture, these results could be driven by some competition between the aromatic compound and the solvent. Nonetheless, similar results have been reported for the adsorption of gaseous benzene in a temperature range of 100-180°C.[24]

Recently, González-Galán and coworkers derived a force field for simulating the adsorption of aromatics on faujasites. They fitted the parameters for reproducing experimental adsorption isotherms of benzene on DaY and NaY.[25] By combining *ab initio* calculations, classical simulations and experimental data, the authors explained how the presence of cation-π interaction pairs could explain why high-silica faujasites are less efficient for separating benzene and cyclohexane.

According to the studies mentioned above, there is a strong evidence of the decisive role of cations on the adsorption process on zeolites. Nevertheless, we have a lack of information about the role played by the amount and the location of the cations. Fulfilling this gap will be useful for designing task-specific zeolites.

The work presented here reports Grand Canonical Monte Carlo simulations for giving an atomistic point of view about the adsorption processes of toluene in faujasites.

2 Computational details

In comparison with other published models,[28] for describing the water adsorption for zeolites with different Si/Al ratio, the forcefield published by Buttefey *et al.*[26] and Di Lella *et al.*[27] (for the same purposes) presents the highest accuracy. Here, we report a set of interaction parameters compatible with the latter model for describing the adsorption of toluene.

2.1 Adsorbent structure

The initial configurations presented in this study were obtained by modifying a NaX structure used in previous works.[29,30] This structure has 86 Na^+ per unit cell, which was the highest cation quantity considered in this work.

By generating other faujasites with a higher Si/Al ratio than to the original one, it was possible to guarantee that the physical-chemistry characteristics of these materials were taken into account correctly. Namely, the Löwenstein rule is obeyed. Second, the relation between preferential site and number of cations is respected. That is to say, for a number of cations less than 32 per unit cell, the Na^+ occupy the so-called sites II. With a cationic quantity higher than 32, but lower than 65, the ions are distributed between the sites I and I' (see Supplementary Material) . Finally, for an even higher quantity of cations, the sites III and III' start to be occupied.[26,27] The only approximation considered here is the indistinguishability between sites I and I' and between III and III'.

This work considered 17 structures and they concern a faujasite framework with a variable number and location of cations. All the systems are listed in Table 1 with the unit cell composition and the population of cation occupying a given site type. The unit cells presented a cubic lattice parameter of 24.8536 Å and duplicated twice in each spatial direction resulting in a 2x2x2 super-cell.

The initial configurations were generated by randomly selecting some cations from the original structure to be preserved, while removing the others. In addition, the closest Al

Table 1: Faujasite structures considered in this work

Zeolite	Composition	N. of Cations	Sites I	Sites II	Sites III
DaY	$Si_{192}O_{384}$	0	0	0	0
NaY2	$Na_2(AlO_2)_2(SiO_2)_{190}$	2	0	2	0
NaY5	$Na_5(AlO_2)_5(SiO_2)_{187}$	5	0	5	0
NaY10	$Na_{10}(AlO_2)_{10}(SiO_2)_{182}$	10	0	10	0
NaY15	$Na_{15}(AlO_2)_{15}(SiO_2)_{177}$	15	0	15	0
NaY20	$Na_{20}(AlO_2)_{20}(SiO_2)_{172}$	20	0	20	0
NaY25	$Na_{25}(AlO_2)_{25}(SiO_2)_{167}$	25	0	25	0
NaY32	$Na_{32}(AlO_2)_{32}(SiO_2)_{160}$	32	0	32	0
NaY40	$Na_{40}(AlO_2)_{40}(SiO_2)_{152}$	40	8	32	0
NaY48	$Na_{48}(AlO_2)_{48}(SiO_2)_{136}$	48	16	32	0
NaY52	$Na_{52}(AlO_2)_{52}(SiO_2)_{140}$	52	20	32	0
NaY56	$Na_{56}(AlO_2)_{56}(SiO_2)_{136}$	56	24	32	0
NaY64	$Na_{64}(AlO_2)_{64}(SiO_2)_{128}$	64	32	32	0
NaX70	$Na_{70}(AlO_2)_{70}(SiO_2)_{122}$	70	32	32	6
NaX76	$Na_{76}(AlO_2)_{76}(SiO_2)_{116}$	76	32	32	12
NaX80	$Na_{80}(AlO_2)_{80}(SiO_2)_{112}$	80	32	32	16
NaX86	$Na_{86}(AlO_2)_{86}(SiO_2)_{106}$	86	32	32	22

atom to the preserved cations is also kept. Notice that the random sampling of cations has been done by respecting the quantity/site population relation discussed previously.

2.2 Force field

2.2.1 Adsorbate-adsorbate interactions

The interactions between toluene molecules are described by using the 10-site model of the TRAPPE force field.[31] This model presents one positive charge at the center of the ring, and two negative charges located at the opposites planes of the ring. In this way, the model can account for the occurrence of cation-π interactions, that have been shown to be relevant for the description of the adsorption process of such compound on zeolites.[25] Figure 2 displays the toluene model representation used: in black, the united atom sites, in blue the positive partial charge and in red the negative charge sites.

Worthwhile to mention, that the partial charges of toluene presented in the original

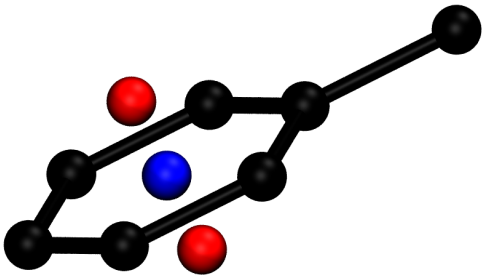

Figure 2: Interaction centers of the toluene molecule: black, united atom centers, blue, positive partial charge, red negative partial charge.

model greatly enhanced the attraction between the adsorbate and adsorbent containing high quantities of cations. This led to a severe overestimation of the adsorption amount at lower pressures. Hence, here we opted for scaling the partial charge values. Several scaling factors were tested for reproducing the experimental adsorption isotherm of toluene on NaY52 reported by Gregis and coworkers.[13] By multiplying the toluene charges by a factor of 0.56, it was found a better agreement with experiments. In addition, the molecule is treated as a rigid entity (no intramolecular degrees of freedom).

Our approach for scaling the charges instead of refitting the other parameters was motivated by the high sensibility of the adsorbed amount to this parameter.[32] Moreover, it was already discussed elsewhere the difficulty of having a transferable non-polarizable potentials for describing the adsorption phenomena.[28,33] It is also important to mention that this represents a more simple procedure than adjusting the Lennard-Jones parameters involving the interaction with cations.

2.2.2 Adsorbent model

The partial charges were retrieved from the work of Buttefey *et al.*[26] and Di Lella *et al.*[27] The authors proposed a linear extrapolation procedure for estimating the partial charges as a function of the number of cations in the structure. The partial charge values for each atom, of the analyzed zeolites, can be found in Table 2. In addition, dispersion interactions involving the zeolite atoms are modeled only with pairs involving either the oxygen atom or the cation.

An important remark to make is that the used model does not distinguish between the Si and Al atoms. In other words, both atoms have the same charge value. Thus, the heterogeneity difference is accounted by recalculating the average partial charge on the oxygen atoms and the tetrahedral centers (Si and Al) for each degree of cation exchange. Here, the charges for the zeolite atoms were obtained using the same interpolation scheme used by Buttefey *et al.*[26] This approximation has already given satisfactory results.[26–28] However, there are other strategies for accounting for the different chemical environments, such as, for instance, distinguishing oxygen atoms connected either to Si or Al. This last strategy was supposed to generate transferable models for zeolites with different degrees of cation exchange.[25,34–36] However, this was proven to be difficult to verify for certain systems.[28]

In our studies, the cations were fixed at the preferential sites. However, for studying dynamical properties (c.f. diffusion) this constraint should preferably be removed.

2.2.3 Adsorbate-adsorbent interactions

We tested two sets of interactions parameters and the simulation results are compared with experimental data for the adsorption of toluene in DaY. The set presenting the best agreement with experimental result is then used to simulate the other faujsites.

The first set of parameters, called set A, was generated by applying the Lorentz-Berthelot mixing rule to the self-interaction parameters of the toluene atom types and of the oxygen atoms of the framework as reported by Di Lella *et al.*[27] The second set of parameters, called

Table 2: Partial charges of the zeolite atoms

Zeolite	q_O	$q_{Si/Al}$	q_{Na}
DaY	-0.800	1.600	-
NaY2	-0.801	1.592	1.000
NaY5	-0.802	1.579	1.000
NaY10	-0.805	1.558	1.000
NaY15	-0.807	1.537	1.000
NaY20	-0.810	1.516	1.000
NaY25	-0.812	1.495	1.000
NaY32	-0.816	1.465	1.000
NaY40	-0.820	1.431	1.000
NaY48	-0.823	1.396	1.000
NaY52	-0.825	1.380	1.000
NaY64	-0.832	1.330	1.000
NaX70	-0.835	1.305	1.000
NaX76	-0.839	1.282	1.000
NaX80	-0.840	1.263	1.000
NaX86	-0.843	1.240	1.000

set B, is derived heuristically and is explained below (details are given in the Supplementary Material).

The parameters developed by Dubbeldam *et al.*, for the interaction of n-alkanes and zeolite atoms have shown to reproduce experimental results for both the adsorption heat and isotherm of alkanes with different chain lengths on zeolites (and with different shapes and sizes).[37] Thus, it is physically acceptable to suppose that these parameters can accurately describe the dispersion interactions, since they largely depend on the volumes of the interacting species. For extracting a plausible value for the interaction parameter for the oxygen of the zeolite, a linear regression was applied between σ_{i-i} and σ_{i-o} parameters for the different atom types. Most of the parameters were taken from Dubbeldam *et al.*,[37] while the σ_{i-i} and ϵ_{i-i} values for the CH_3 and CH_2 atom types, were taken from the GROMOS forcefield.[38,39] It was shown that this model has the best accuracy in describing the interactions between n-alkane molecules.[40,41] By considering an arithmetic mean, the σ_{o-o} parameters are calculated as twice the value of the intercept obtained by this regression. Then, the arithmetic

mean between this new value of σ_{o-o} and the σ_{i-i} given by the TRAPPE model was used to obtain the σ_{i-o}.

A different procedure was used for estimating ϵ_{o-o}. Given σ_{o-o}, σ_{i-i} and ϵ_{i-i}, different values for ϵ_{o-o} can be obtained by applying Equation 1,[42] where $i = CH_4, CH_3, CH_2, CH$ and C. The final estimate for ϵ_{o-o} is obtained by averaging the values obtained for the different pairs. The ϵ_{i-o} interaction parameters between the toluene atom types (given by the TRAPPE model) and the oxygen of the zeolite were obtained by applying the same mixing rule. This size-weighted mixing rule improves the accuracy of adsorption simulations.

$$\epsilon_{ij} = \frac{1}{2}\left(\frac{\sigma_i}{\sigma_j}\epsilon_i + \frac{\sigma_j}{\sigma_i}\epsilon_j\right) \tag{1}$$

The interactions between the cations and the atom of the toluene molecule have been modeled by using the Dang[43] (for Na^+) and the TRAPPE model (for the toluene molecule) and followed by the Lorentz-Berthelot mixing rule (Tables 3 and 4). A cut-off radius of 12 Å was applied to the pairwise interactions and periodic boundary conditions in the three directions. The Ewald sum is used for treating the long-range contributions to the electrostatic interactions.

Table 3: Lennard-Jones Interaction Parameters

Atom type	Description	σ_{ii} (Å)	ϵ_{ii} (K)	q	Reference
CH_3	Methyl site	3.750	98.00	0.00	[31]
CH	Aromatic CH site	3.740	48.00	0.00	[31]
C	Aromatic C bonded to methyl site	3.880	21.00	0.00	[31]
CM	Charge site at the center of ring	-	-	1.3552	This work
M	Charge site on top and below ring	-	-	-0.6776	This work
Na^+	Sodium cation	2.584	50.27	Table 2	[43]
Si	Zeolite Silicon	-	-	Table 2	[26,27]
Al	Zeolite Aluminum	-	-	Table 2	[26,27]
O_A	Zeolite Oxygen (set A)	3.000	93.53	Table 2	[26,27]
O_B	Zeolite Oxygen (set B)	3.855	57.43	Table 2	This work

Table 4: Cross interaction Lennard-Jones Parameters

Interaction pair	Set A		Set B	
	σ_{ij} (Å)	ϵ_{ij} (K)	σ_{ij} (Å)	ϵ_{ij} (K)
CH3-O	3.375	95.74	3.480	93.00
CH-O	3.370	67.00	3.868	39.10
C-O	3.440	44.32	3.798	52.88

2.3 Monte Carlo simulations

For calculating the adsorption isotherms, the GPU Optimized Monte Carlo (GOMC) code version 2.70[44] was used to carry on the simulations in the μVT ensemble and the Configurational-bias Monte Carlo method.[45] By imposing a chemical potential, the average number of adsorbed molecules is measured directly. The simulations are performed at 298.15 K and the fugacities range from 0.1 to 2500 Pa. Henceforth, the adsorbed amount reported in this work refers to the absolute adsorbed amount.

The proportion of Monte Carlo moves were: 0.1 translation; 0.1 rotation; 0.1 intrabox swaps (this move consists of exchanging the position of two molecules already inside the simulation box); 0.7 insertion. Moreover, an exclusion distance of 0.5 Å was used to prevent the occurrence of nonphysical configurations. The simulation length is of 5×10^7 Monte Carlo steps for the zeolites having less than 70 cations. For the other systems (*e.g.*, $NaX_{(70\text{-}86)}$), 6×10^7 steps are used. In the simulations the last 1×10^7 iterations are used as production data. The input files were generated with the aid of the MoSDeF utilities[46–48] (see Supplementary Information). The equilibration state was determined by the convergence of an average value of both the adsorbed amount and total energy.

2.4 Simulation analysis

In this work we compared the adsorption processes of the systems given in Table1 by analyzing: the adsorption isotherms, calorimetric heat of adsorption, radial distribution functions, occupancy maps and the total amount of interacting pairs formed between the toluene

molecules and the cations. This last quantity was defined by the number of toluene molecules for which the ring center are located below 3.3 Å from a cation. For the structural quantities, the VMD software[49] was used.

For extracting the adsorption isotherm, one has to calculate the average amount of adsorbed molecules at the production runs, and relate the fugacity of the adsorbate with the pressure for drawing the comparison with experimental results. Here, it was considered that the gas obeys the ideal gas law, which is a reasonable assumption at these conditions.

For calculating the calorimetric heat of adsorption, two approaches are used. One based on the fluctuations given by Equation 2. In this equation E_{tot} is the total energy of the system, N is the number of the toluene molecules of the system, T is the temperature, R is the universal gas constant and the brackets refer to the ensemble averages.

$$\Delta H_{ads} = RT - \frac{\langle E_{tot} N \rangle - \langle E_{tot} \rangle \langle N \rangle}{\langle N^2 \rangle - \langle N \rangle^2}. \tag{2}$$

Notice that this method may fail for poor statistics at low loadings. This can be overcome by producing very long simulations to reduce the numerical noise and for having reliable averages. It has been reported that such procedure may be impractical at very low chemical potentials.[50] Hence, a second procedure has been employed based on the intermolecular energy (E_{inter}) given by:

$$E_{inter} = \frac{\langle E_{tot} \rangle - \langle E_{intra,tol} \rangle - E^o_{framework}}{N_{cells}}, \tag{3}$$

with N_{cells}(=8) stands for the number of unit cells, $E_{intra,tol}$ is the intramolecular energy of the toluene molecules and $E^o_{framework}$ is the total energy of the empty framework at the beginning of the simulation. Given that, the cations were held fixed $E^o_{framework}$ is the intramolecular energy of the framework (that is constant for the entire simulation).

A molar potential energy of adsorption ($\Delta U_{mol,ads}$) can be defined as the derivative of

$\langle E_{inter} \rangle$:

$$\Delta U_{mol,ads} = \frac{\mathrm{d}\langle E_{inter} \rangle}{\mathrm{d}\langle N_{(ads.U.C.)} \rangle}, \tag{4}$$

where $\langle N_{(ads.U.C.)} \rangle = \langle N/N_{cells} \rangle$ is the number of adsorbed molecules per unit cell. By assuming that the gas phase behaves as an ideal gas, it is possible to relate $\Delta U_{mol,ads}$ to the calorimetric heat using the relation:

$$\Delta H_{mol,ads} = \Delta U_{mol,ads} - RT. \tag{5}$$

3 Results and discussion

3.1 Model validation

Before discussing how the different amount of cations influence the adsorption some comparisons with experimental results are given for justifying the parameters used. Figure 3 displays the accuracy of the sets given in Table 4 for reproducing the experimental results from Pujol *et al.*,[51] for the structure $Na_2(AlO_2)_2(SiO_2)_{190}$.

Clearly, set B outperforms set A. Not only the onset of the adsorption is closer to the experimental data for set B, but also set A seems to present a saturation plateau at lower pressures than the saturation pressure. Specifically, set A results in a too-early onset of adsorption saturation. This last is absent for set B which exhibits an enhanced agreement with experimental results near the saturation pressure ($\approx$ 3800 Pa). This result suggests that the heuristics employed here to derive the σ_{o-o} and ϵ_{o-o} parameters is reasonable (see subsection 2.2.3). Its justification would reside in the use of cross-interaction parameters that present a good description of the dispersion interactions and the use of a mixing rule that better describes the interactions of atoms with large difference on the value σ parameter of the interaction potential.

Worthwhile to mention that the presence of the inflection point and the rapid increase

in the adsorbed amount around tens of Pa was also reported by Zheng and coworkers.[52] The authors explained this fact by a change in the mechanism of adsorption. While at low loads, the aromatic molecules adsorb at an ideal site near the cage surface, the fourth additional molecular must be inserted elsewhere between the already adsorbed molecules. Thus changing the interactions and location sites involving the adsorption process, which in consequence modifies the shape of the isotherm.

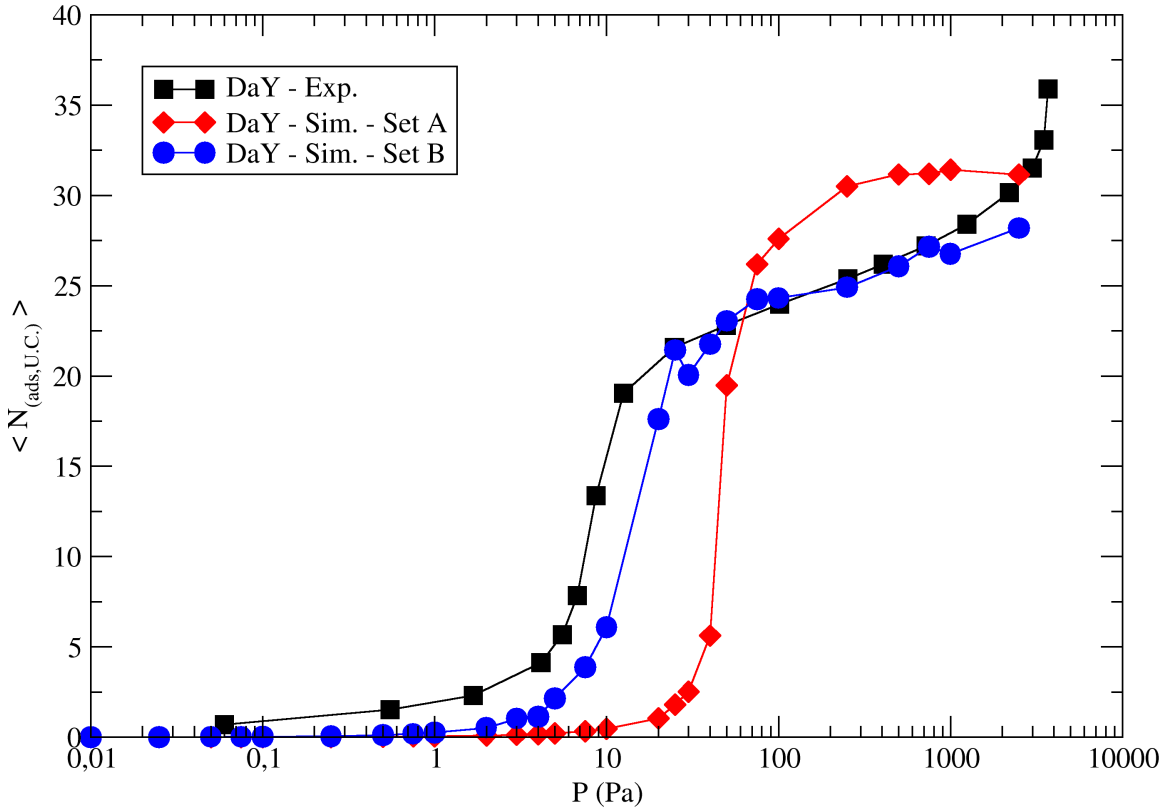

Figure 3: Comparison of the adsorption isotherm obtained at 298.15 K with the parameters given in Table 4.

For completing the validation of our model, it was necessary to evaluate its accuracy for reproducing experimental results from cation-exchanged zeolites. Thereupon, the simula-

tions are compared with experimental adsorption isotherms for toluene on NaY (composition $Na_{52}(AlO_{52})_2(SiO_2)_{138}$) at 298.15 K from Gregis *et al.*[13]

Figure 4 shows that by using the original partial charges of the toluene model the agreement is far from being satisfactory. Therefore, we opted for a scaling of the partial charges. In this manner, the agreement was improved and the model continues to be compatible with the parameters of Buttefey *et al.*[26] and Di Lella *et al.*[27]

Different scaling factors for the partial charges of the toluene molecule were tested in a 1x1x1 cell and the best results are obtained with a factor of 0.56. Figure 4 shows the improved accuracy of the model for NaY52, while only having minor effects on the DaY-toluene systems. Henceforth, it is reasonable to assume that this charge scaling factor can be used to describe the interaction of the toluene molecule with faujasites with different degrees of cation exchange. Moreover, such results suggest that the adsorption of toluene on DaY is governed mainly by dispersion interactions.

Remark that this scaling factor is an adjusted parameter for the system considered here and probably should be refined for different systems. The discussion of its physical meaning, if any, is out of the scope of this work. The argument advocating in favor of the approach used is that the need for rescaling the charges reflects the difficulty of deriving accurate transferable and non-polarizable models for describing the adsorption process.

Figure 5 gives the heat of adsorption for DaY, NaY56 and NaX86 by using Eq.2 and Eq.5, they show a good agreement with those reported by F. Benoit[53] and E. Pilverdier.[54] Although the values calculated with Eq.2 are in agreement within the experimental data for DaY they overestimates the heat of adsorption for NaY. Notice that, some of the experimental features are observed in the simulations as well. Namely, the increase of the heat of adsorption as a function of the adsorbed molecules for DaY. The pronounced decrease of heat of adsorption observed experimentally and by simulations may be associated to condensation of molecules.

For verifying if the interactions between the aromatic ring and cations are well described, we calculated the radial distribution function, $g(r)$, between the center of the aromatic ring

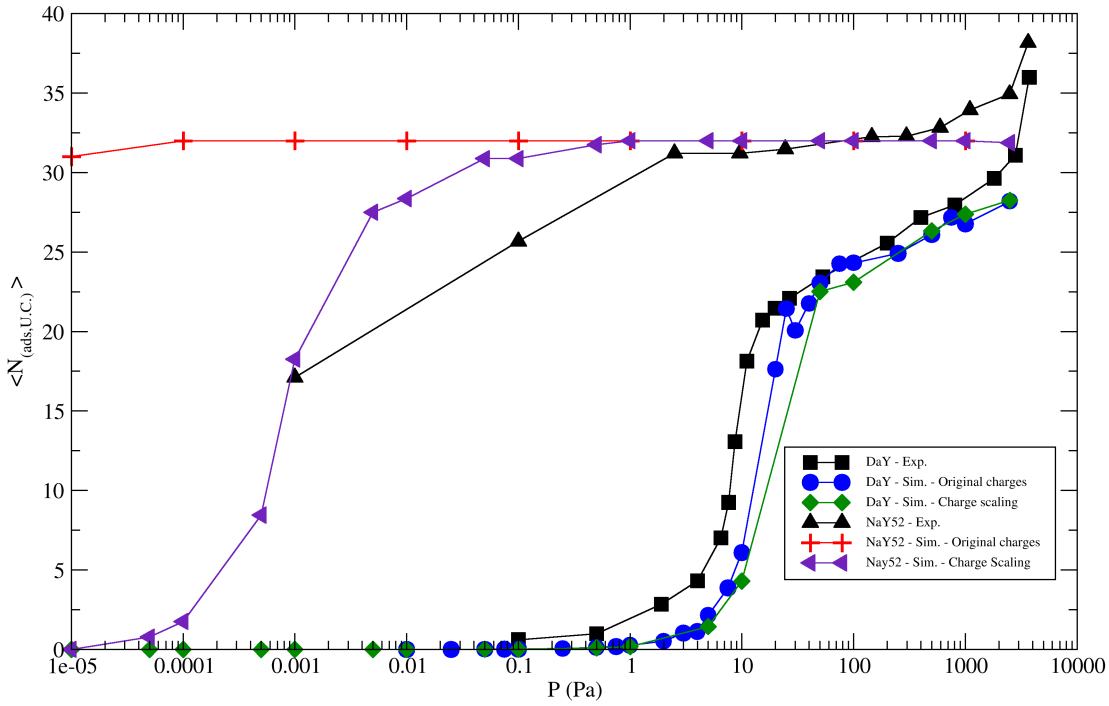

Figure 4: Comparison of the adsorption isotherms obtained at 298.15 K with the original charges of the toluene model of the TRAPPE forcefield[31] and with the charges scaled by 0.56. As can be seen the scaling does not change results for DaY, while it enhances the agreement with experiments for NaY52.

and the cations located at each site separately. Figure 6 gives the results for NaX86 (at 1000 Pa), we can observe the presence of a pronounced peak around 2.5 Å involving the cation at site III. This value is in agreement with electronic structure calculations of cation-π complexes[55] and observed within the faujasite framework.[25]

Another interesting feature in Figure 6 is the smaller peak at 3.0 Å involving cations located at site II. This suggests that either toluene molecules interacting with these cations are less tightly bonded or that cations at site III modulate such interactions. In addition, no interacting pairs are present between toluene and cations located at site I, which is related to the fact that such ions are less accessible.

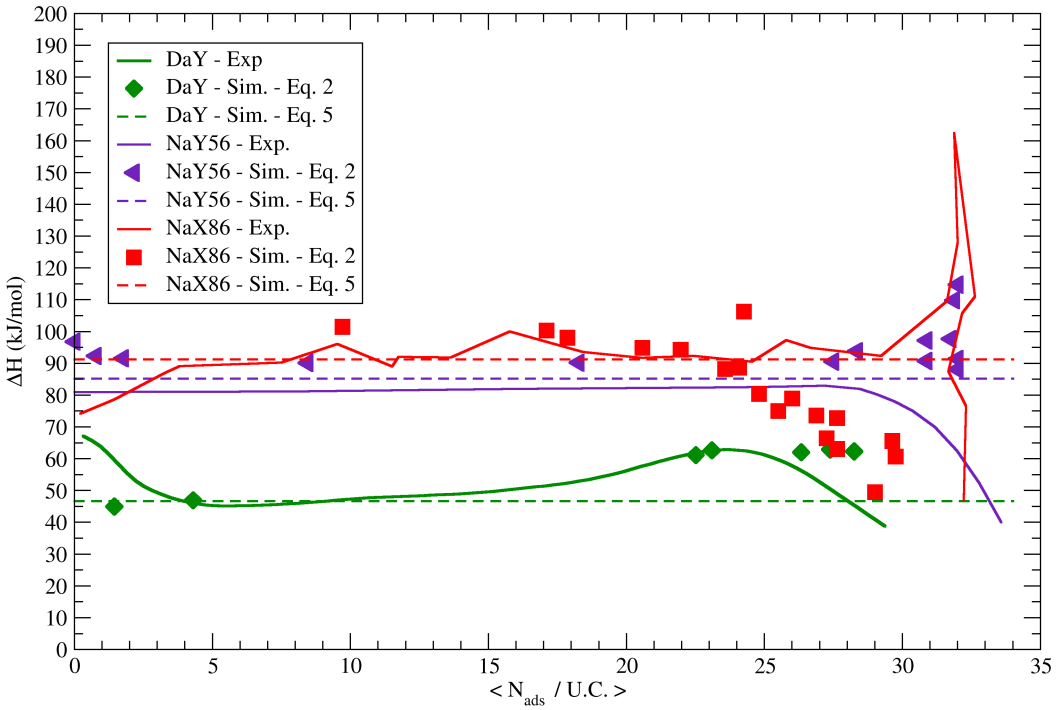

Figure 5: Comparison between experimental and calculated heats of adsorption at 298.15 K by using Equations 2 and 5.

3.2 The cumulative effect of cations in different sites

The comparison between the different cation-exchanged faujasites begins by analyzing zeolites without cations (DaY), with cations only on site II (NaY32), with cations on sites I and II (NaY64) and with cations on the three sites (NaX86). The obtained adsorption isotherms are displayed in Figure 7.

Our simulations show that cations increase the adsorption amount. It is interesting to observe that NaY32 and NaY52 saturates both around 32 molecules per unit cell, while NaX86 does not seem to reach a saturation plateau. Notice that the NaX86 adsorbs more molecules at low pressures ($<$ 0.004 Pa) than the NaY(32-52). However, as loading is increased this tendency is reversed. This last is in agreement with experimental results reported for the adsorption of gaseous benzene[24] and for toluene diluted in octane.[23]

The isotherms for DaY and NaY32 show that the presence of cations in site II produce

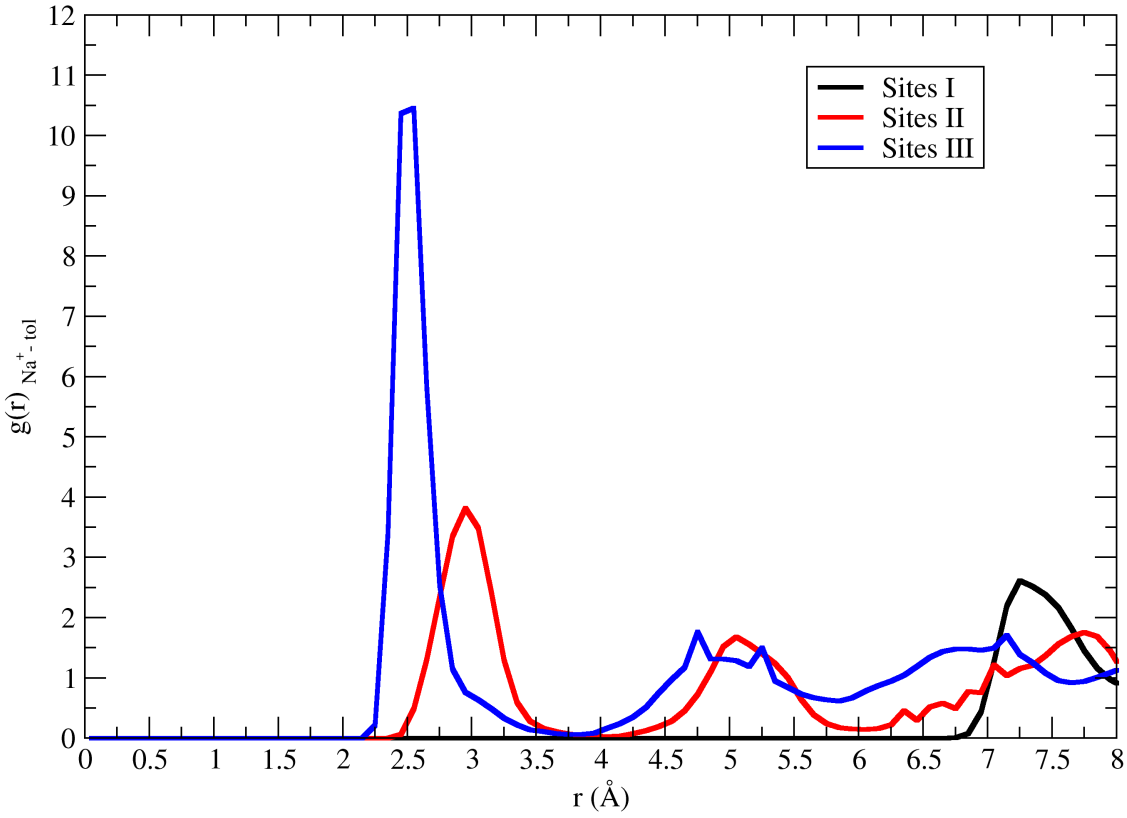

Figure 6: Pair distribution functions for toluene and Na^+ (NaX86 at 1000 Pa). The curve was calculated considering the center of the aromatic ring and the cations located at each site separately.

an increase of adsorption and for the structures NaY(32-52) we can say that cations on site I have a minor effect on the adsorption process.

The main difference between structures NaY(32-52) and NaX86 is the presence of cations in site III for the latter structure. Figure 7 suggests that the presence of these cations enhance the adsorption at lower pressures but hinders it when the pores are already occupied.

The different amount of cations and their location gives rise to a different charge distribution for each faujasite and gives place to the formation of different kind of interacting pairs. These implies that the interaction energies and the spatial organization of the adsorbed

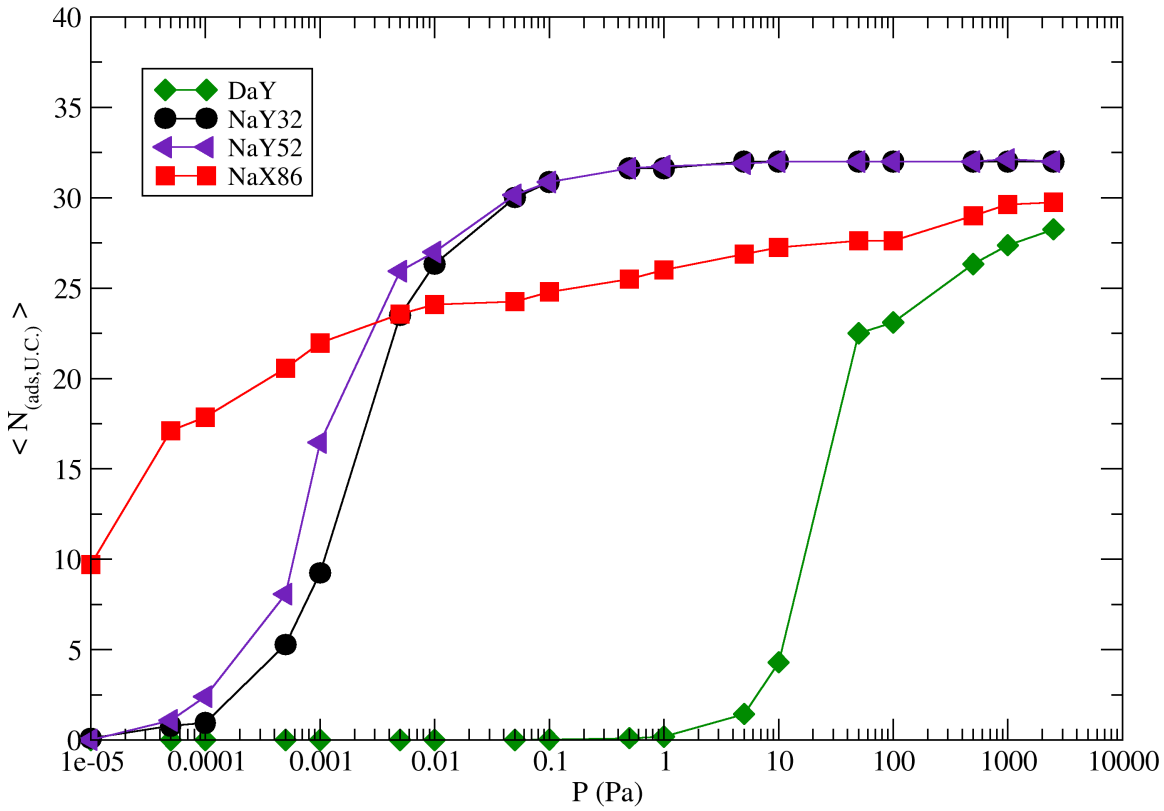

Figure 7: Adsorption isotherms at 298.15 K for toluene on DaY, NaY32, NaY52 and NaX86.

molecules will be different.

Figure 8 gives $\langle E_{inter} \rangle$ as a function of the adsorbed molecules and presents a linear trend. The figure shows that DaY (without cations) is the one having a less negative slope. The structures NaY32 and NaY52 have a rather similar slope . This suggests that cations on site II are energetically determinant for adsorption, even when sites III are the most energetically favorable as indicated by the deepest slope of the NaX86. The calculated attractive interactions in NaX86 might be associated to the formation of cation-π complexes and can explain its earlier onset of the adsorption.

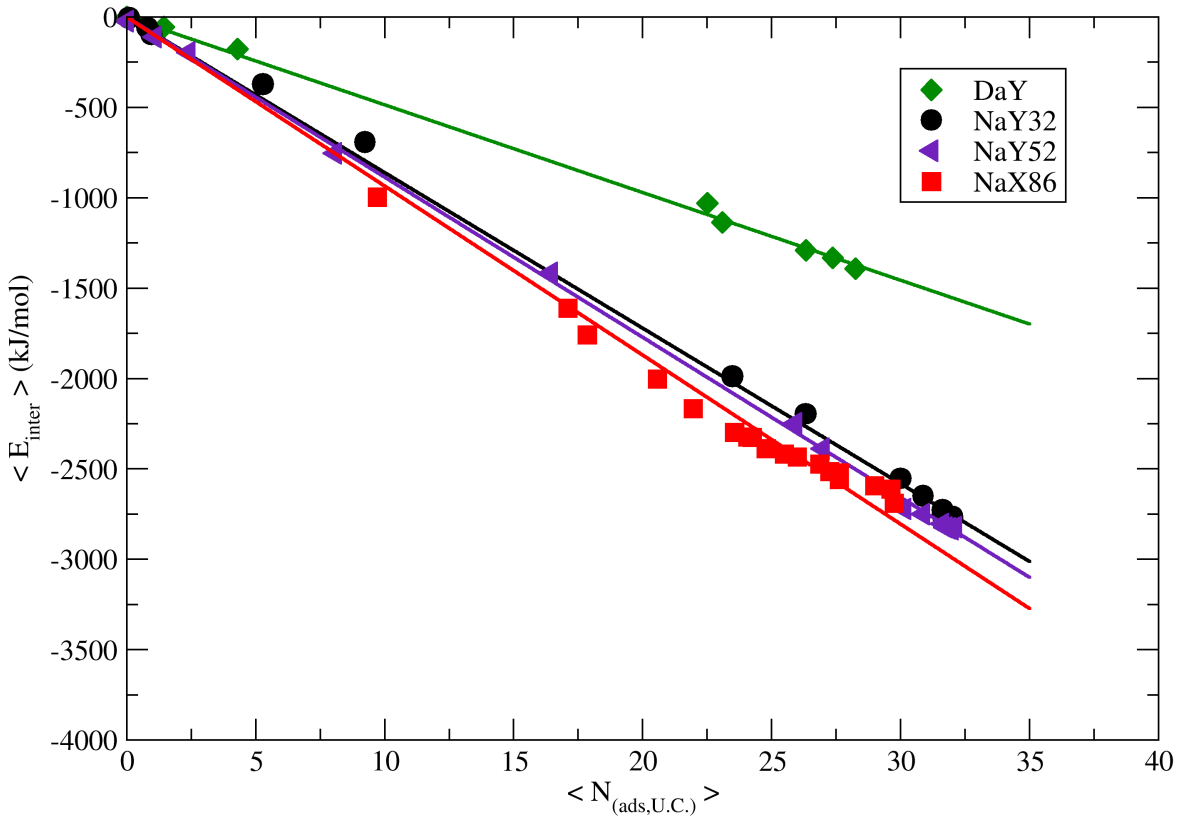

Figure 8: Internal energy (in kJ per mol) as a function of the number of adsorbed molecules of toluene on DaY, NaY32, NaY and NaX

3.3 The effect of increasing the number of cations at site II

Next, we proceed to analyze the effect of varying the number of cations at site II. According to the literature,[26,27] when the number of cations do not exceed 32 per unit cell, the ions would be located at site II. Figure 9 compares the adsorption isotherms of toluene on faujasites with a degree of cation exchange smaller than 32. A small number of cations, e.g., 2 or 5 per unit cell, is already enough to shift the adsorption curve towards lower pressures. In addition, there is a trend to increase the adsorption with the number of cations at site II. Moreover, as the number of cations is increased, the interaction energy between the framework and the

adsorbate becomes more attractive. This last is shown in Figure 10 that gives the molar internal energy of adsorption ΔU_{ads} as a function of the number of cations. By taking the derivative of the previous figure, it is easy to show that the highest variations will be between 0 to 32 cations (corresponding to the points with the higher steep).

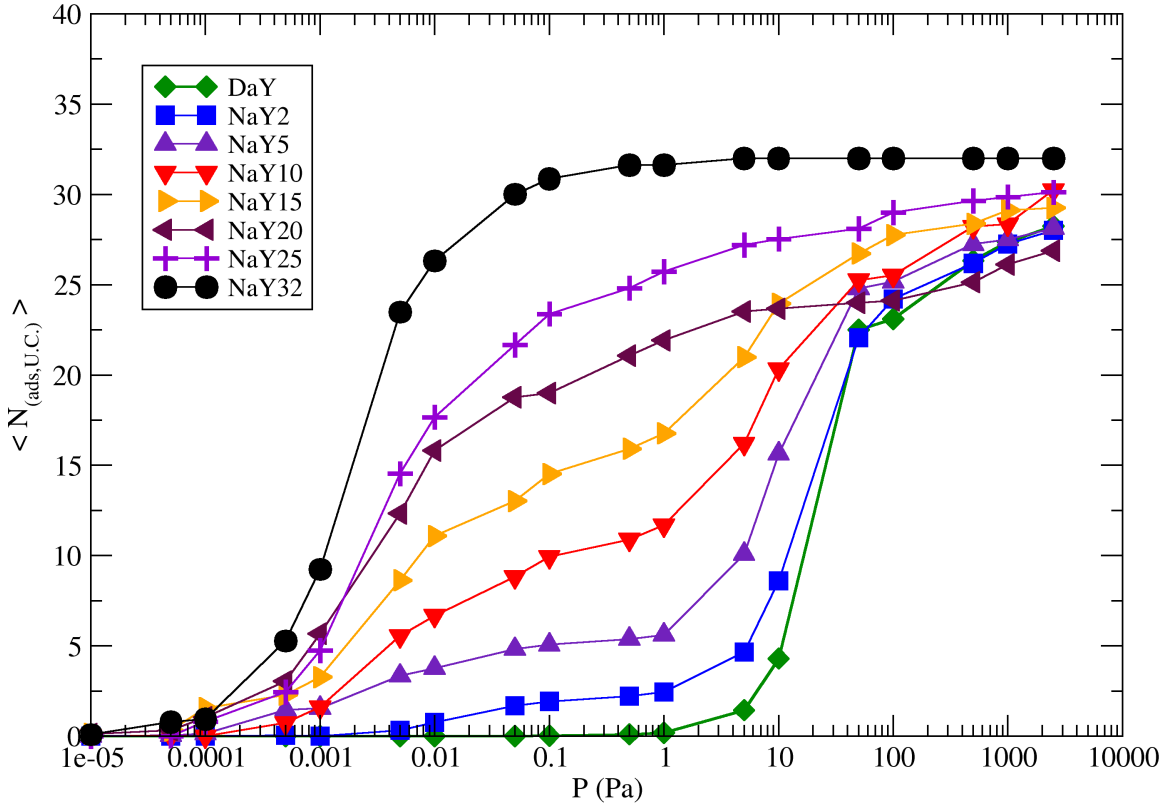

Figure 9: Adsorption isotherms at 298.15 K of toluene on faujasites containing cations on site II.

Let us discuss in detail the form of the adsorption curves in Figure 9. The change on the steepness of the curves can be explained by making use of the occupation of cationic sites by toluene molecules. In the y-axis of Figure 11 is given the average fraction of adsorbed toluene molecules occupying a cationic site. This is calculated by taking the ensemble average of the

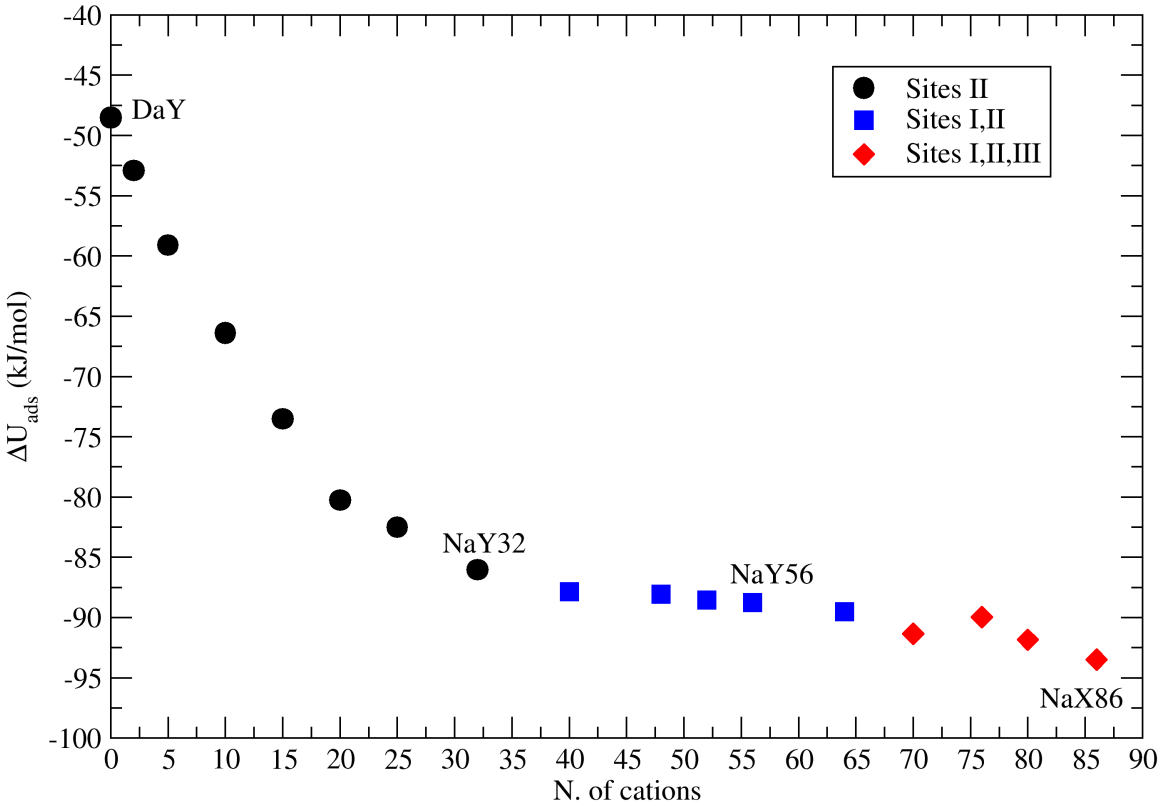

Figure 10: Internal energy of adsorption as a function of the number of cations for the faujasites analyzed (See Table 1).

ratio between the number of toluene molecules within a distance of 4Å from the cation and the total number of adsorbed toluene molecules ($\langle N_{(pairs,tol-cat)}/N_{(ads,U.C.)}\rangle$). The decreasing value of this ratio means that all the cationic sites are linked to an adsorbed molecule and subsequent molecules find their equilibrium positions in the free available space of the supercage. Intriguingly, the starting points of the decay in Figure 11 (*e.g.* in NaY15 the decay starts at $\langle N_{(ads,U.C.)}\rangle \approx 15$) coincides with the change of adsorption regime (Figure 9). Hence, we may conclude that adsorption begins by first saturating the cationic sites.

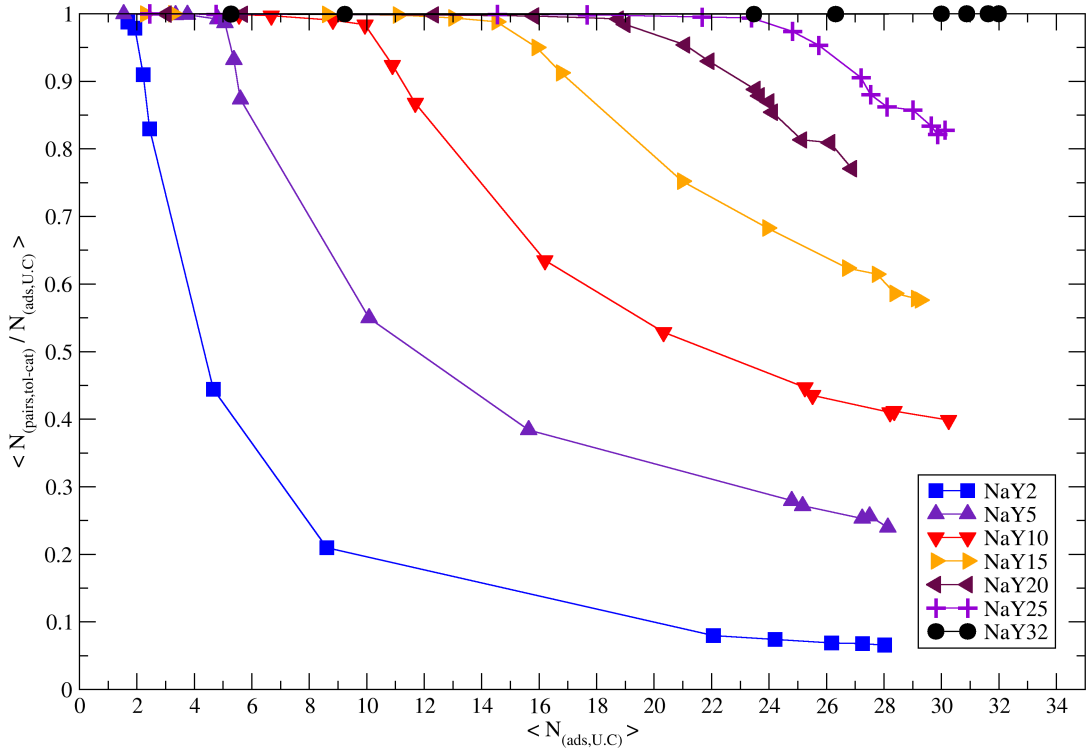

Figure 11: The fraction of toluene molecules interacting with a cation on site II for faujasites NaY2-32.

3.4 The effect of increasing the number of cations at site III

The adsorption isotherms for structures with cations on site III are displayed in Figure 12. These cations imply a shift of the adsorption process at lower pressures. One may expect that by increasing the amount of cations on site III may induce an increase of the adsorbed molecules, since the molar internal energies of adsorption for these frameworks are the most favorable (Figure 10). However, Figure 12 shows that NaY64 (i.e.,cations on site I and II) adsorbs the most at higher pressures. This apparent contradiction, as it is discussed below, is due to a steric hindrance induced by cations on site III.

Given that, the hindering of adsorption at higher pressures occurs in faujasites containing cations at site III, specific interactions between the toluene and these cations might play a decisive role on the origin of the steric hindrance. In Figure 13 is given the comparison of the $g(r)$ involving center of the toluene rings and cations for different zeolites. The $g(r)$

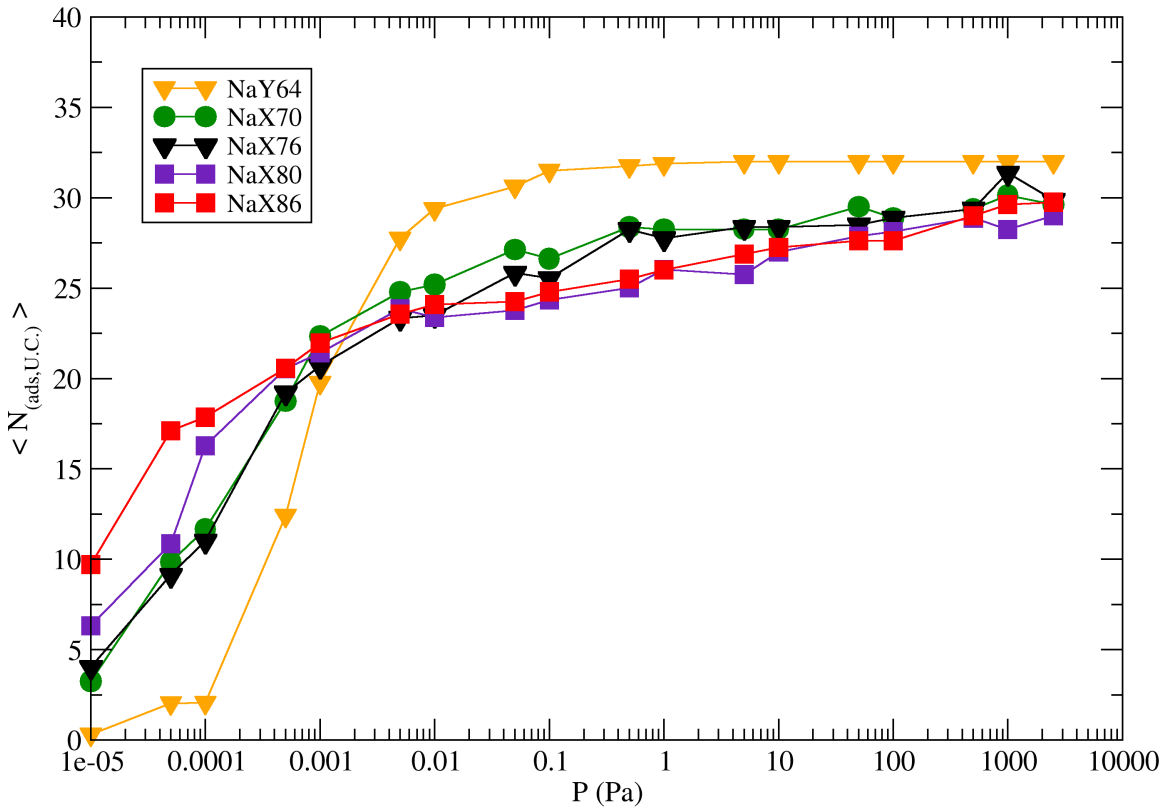

Figure 12: Adsorption isotherms at 298.15 K of toluene on faujasites containing cations on sites I, II and III.

for cations at site II present a peak at the same distance as for NaY64 (green solid line) and NaX86 (red solid line). This interaction produces an organized arrangement of toluene molecules (see inlets in Figure 13). The $g(r)$ for the cations at site III of the NaX86 is shifted to the left by 0.5 Å. This implies that toluene molecules interact preferentially with cations on site III and they disturb the arrangement of the toluene molecules. More details can be evoked to explain such results, by analyzing the fraction of toluene molecules occupying a given site, see Figure 14. At low loadings, the toluene molecules are preferentially attached to site III cations. This reflects the higher exposition of the adsorbate molecules to these sites

and its high attractivity. As loading is increased, a competition of the two sites for adsorbing the aromatic molecules starts. The number of adsorbate molecules interacting with the site II cations increases and simultaneously decreases the fraction of aromatic molecules adsorbed near site III.

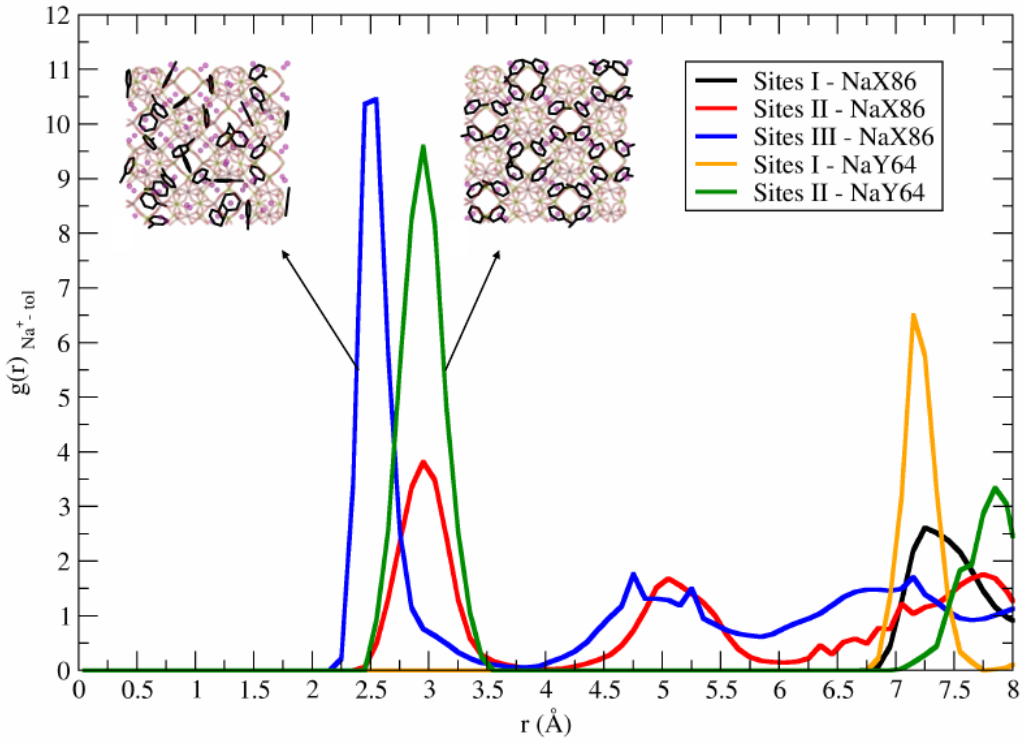

Figure 13: Radial distribution function between the center of the ring and the cations of each site.

If one compares the NaY and NaX systems, for the latter the toluene molecules are less restraint to the cations on site II. This is probably due to the strong interactions between the adsorbate and cations at site III. This explanation is in agreement with the Vitale *et al.*[56] neutron diffraction experiments for NaX with a low coverage of benzene. The authors claimed that the presence of cations at site III changes the relative stability of other adsorption sites.

Figures 15a and b display the last configuration for zeolites NaY with cations on site II - only- and on sites I and II, respectively. They show an organization pattern of the toluene molecules. This pattern is formed by the aromatic ring located parallel to rings containing a cation at site II. A similar adsorption pattern has been observed experimentally by Fitch

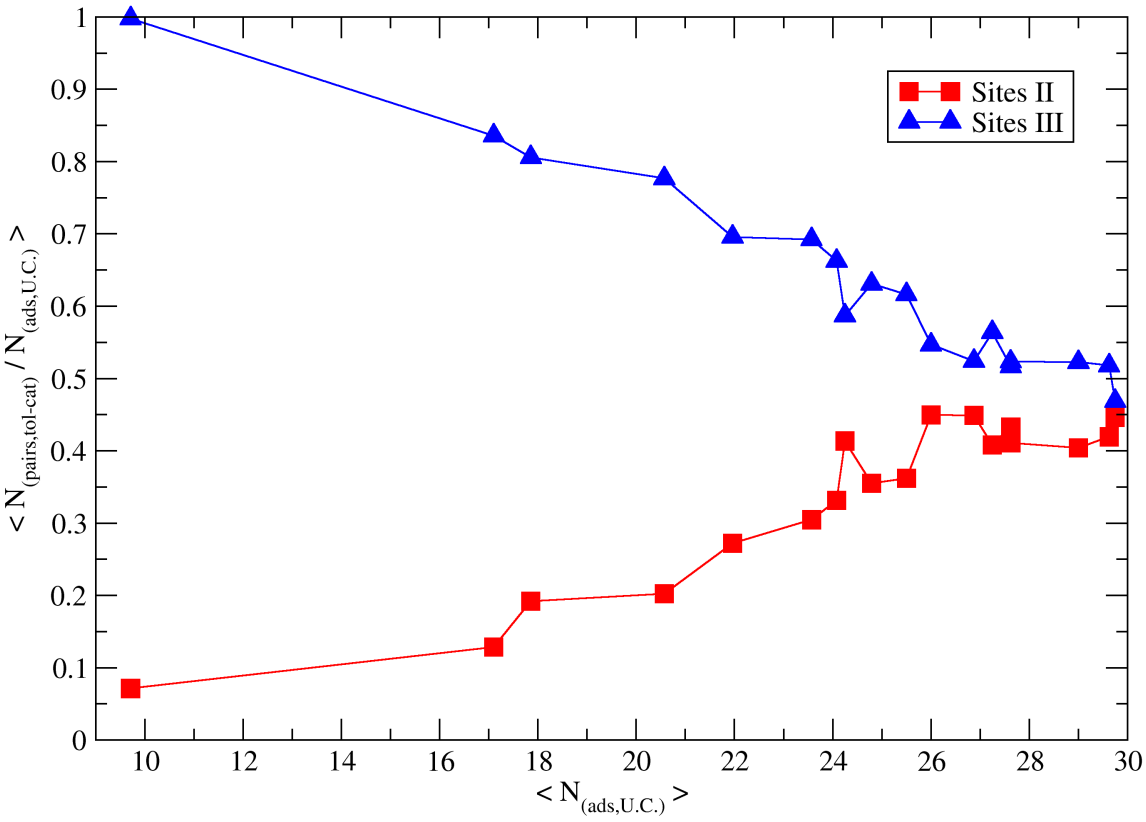

Figure 14: The fraction of toluene molecules interacting with a cation on site II (red squares) and with a cation on site III (blue triangles) for NaX86 at 1000Pa.

et al.[14] for the adsorption of benzene molecules. This molecular arrangement seems to be a robust result since it has been observed by other computational studies in all-silica faujasite and for HY zeolites.[52,57] Moreover, such observations also point out to the fact that the mobility of cations would not have a significant impact on the results reported here. Figures 15c and d correspond to faujasite NaX with an increasing number of cations on site III. They clearly show that the organized pattern is destroyed by the presence of these last cations.

Our results suggest that the formation of organized patterns depends on the spatial and orientational freedom of the toluene molecules in the vicinity of site II. By being less restraint

to the sites II (*i.e.*, inclusion of cations on site III), the toluene molecules may be subject to higher steric hindrance inside the cage, which, according to Daems and coworkers[23] will reduce the adsorption of molecules. This is shown by the average occupations maps in Figure 16. The depicted black surfaces correspond to the average spatial occupation of toluenes obtained from the total number of configurations. In faujasites having cations on site II and III (Figures 16c,d), the toluene molecules spread out a larger occupation area than in NaY32 and NaY64 (Figures 16a,b that do not contain cations on site III). This is translated as an impediment for the optimum packing of adsorbate molecules inside the cage.

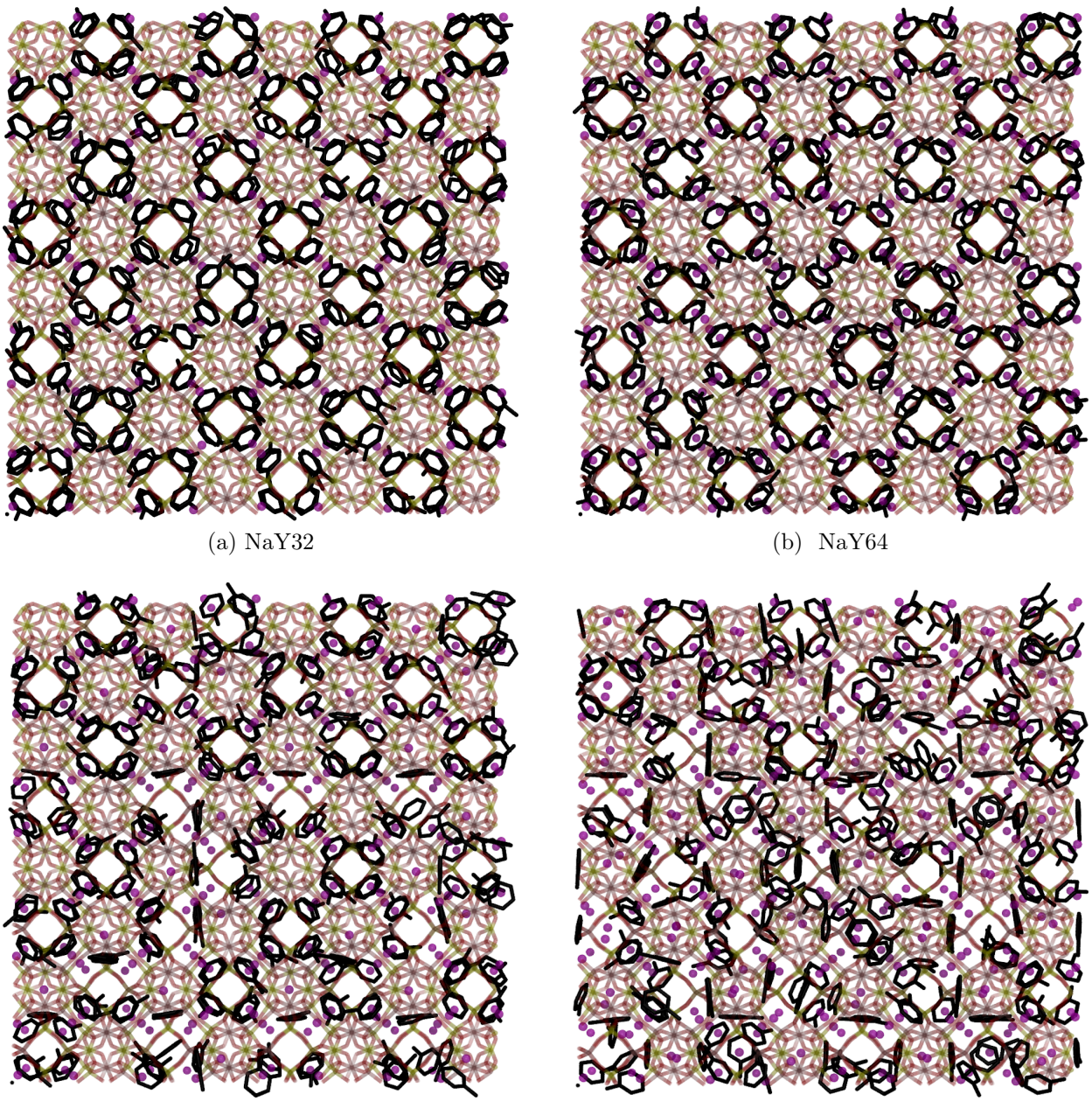

(a) NaY32 (b) NaY64

(c) NaX70 (d) NaX86

Figure 15: Configuration snapshots of adsorbed toluene molecules for (a) NaY32, (b) NaY64, (c) NaX70 and (d) NaX86.

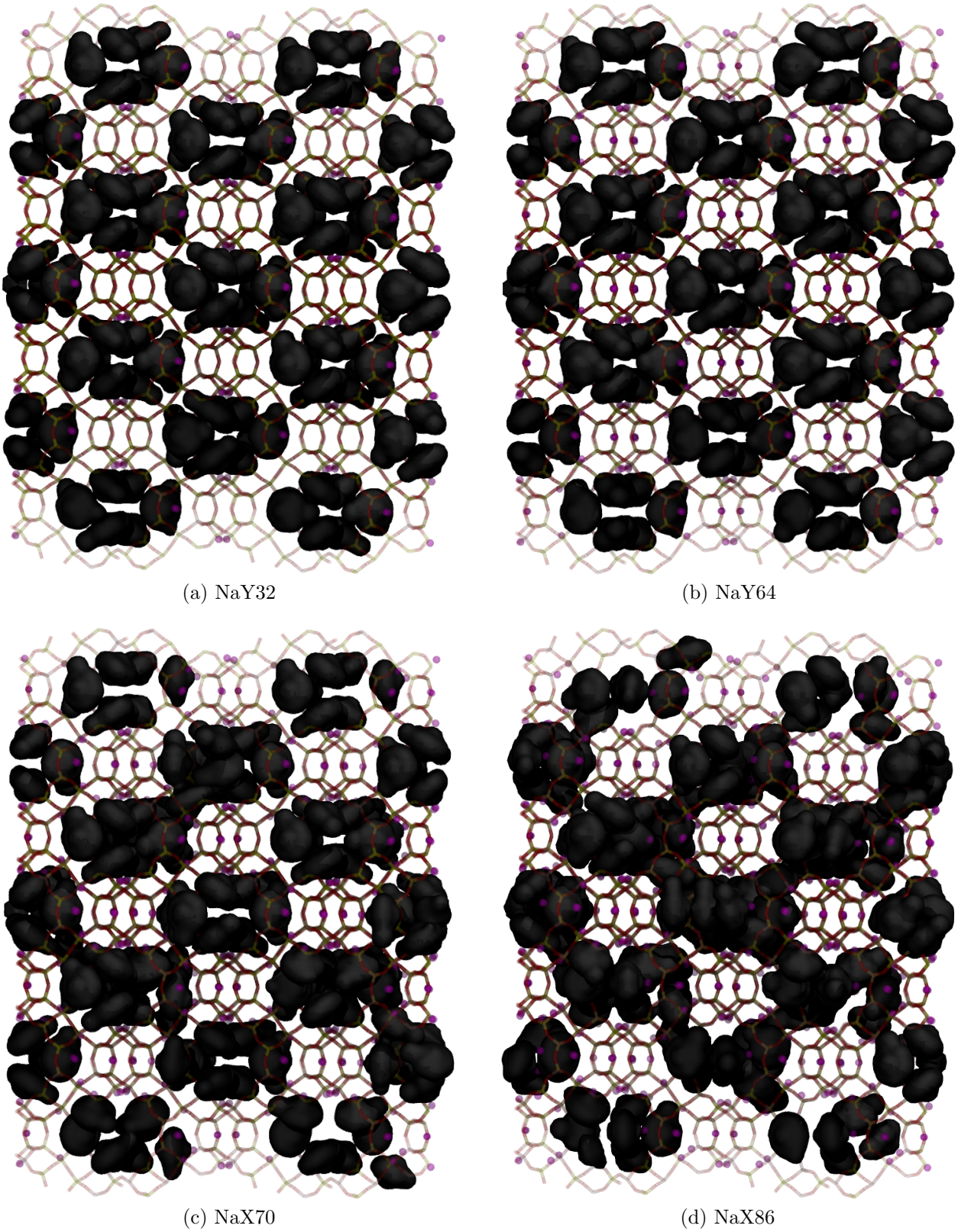

(a) NaY32 (b) NaY64

(c) NaX70 (d) NaX86

Figure 16: Average spatial occupations maps of toluene molecules for (a) NaY32, (b) NaY64, (c) NaX70 and (d) NaX86.

4 Conclusions

The cations inside a zeolite according to their quantity and location generate specific interactions, that will govern the adsorption processes. Their understanding is undoubtedly necessary for engineering novel devices (e.g., captors).

The studies reported here give a set of interaction parameters for describing the interaction of toluene with faujasites with a variable Si/Al ratio. They are compatible with an already published model for the adsorption of water in faujasites.

The model revealed some interesting features. As more cations occupy site II, the lower are the pressures for initiating the adsorption process. These cations are responsible for making the interaction energy between the toluene and the framework more attractive. The cations on sites I do not shown a significant influence on the adsorption process. The cations on site III are responsible for increasing the adsorption at low pressures but as loading is increased they render it more difficult. This last is due to the fact that these cations produce a steric hindrance. We observed that the toluene molecules interact differently with cations on sites II and III. In consequence, there will be a competition between those sites for forming interaction pairs with the adsorbate. Our simulations show that such competition enhances the steric hindrance and deteriorates the toluene organization (induced by sites II) inside the cages.

The Si/Al ratio is related to the hydrophobicity of the zeolite. Higher ratios (less cations) represent frameworks less prone to adsorb water molecules. However, such systems do not present a sensibility towards toluene. Thus, a perspective work would consist of performing computational studies to understand the competitive adsorption between toluene and water on faujasites. This would enable, for instance, finding an optimum Si/Al ratio that could adsorb the aromatic compound with high sensibility, while preserving its selectivity in relation to water. This last could be of practical use in applications ranging from pollution control to cancer diagnostic procedures.

5 Acknowledgments:

We thank the CRI-CCUB Université de Bourgogne for giving us access to the computing facilities. We thank the EUR EIPHI and the region Bourgogne-Franche Comté for financial support.

References

(1) World Health Organization(WHO), *Toluene*; Environmental Health Criteria; World Health Organization: Genève, Switzerland, 1986.

(2) da Silva, C. M.; Corrêa, S. M.; Arbilla, G. Preliminary Study of Ambiente Levels and Exposure to BTEX in the Rio de Janeiro Olympic Metropolitan Region, Brazil. *Bulletin of Environmental Contamination and Toxicology* **2020**, *104*, 786–791.

(3) United States Department of Labor - Occupational Safety and Health Administration: Toluene. Website, 2022; `https://www.osha.gov/toluene/occupational-exposure-limits`.

(4) Directive 2008/50/EC of the European Parliament and of the Council of 21 May 2008 on ambient air quality and cleaner air for Europe. Website, 2015; `http://data.europa.eu/eli/dir/2008/50/2015-09-18`.

(5) Kim, K.-H.; Szulejko, J. E.; Raza, N.; Kumar, V.; Vikrant, K.; Tsang, D. C. W.; Bolan, N. S.; Ok, Y. S.; Khan, A. Identifying the best materials for the removal of airborne toluene based on performance metrics - A critical review. *J. Clean. Prod.* **2019**, *241*, 118408.

(6) Wang, W.; Ma, X.; Grimes, S.; Cai, H.; Zhang, M. Study on the absorbability, regeneration characteristics and thermal stability of ionic liquids for (VOCs) removal. *Chem. Eng. J.* **2017**, *328*, 353–359.

(7) Vellingiri, K.; Kumar, P.; Deep, A.; Kim, K.-H. Metal-organic frameworks for the adsorption of gaseous toluene under ambient temperature and pressure. *Chemical Engineering Journal* **2017**, *307*, 1116–1126.

(8) A geometric solution to the largest-free-sphere problem in zeolite frameworks. *Microporous and Mesoporous Materials* **2006**, *90*, 32–38, Dedicated to the late Denise Barthomeuf, George Kokotailo and Sergey P. Zhdanov in appreciation of their outstanding contributions to zeolite science.

(9) Kraus, M.; Trommler, U.; Holzer, F.; Kopinke, F.-D.; Roland, U. Competing adsorption of toluene and water on various zeolites. *Chem. Eng. J.* **2018**, *351*, 356–363.

(10) Lv, Y.; Sun, J.; Yu, G.; Wang, W.; Song, Z.; Zhao, X.; Mao, Y. Hydrophobic design of adsorbent for VOC removal in humid environment and quick regeneration by microwave. *Microporous and Mesoporous Materials* **2020**, *294*, 109869.

(11) Hunter-Sellars, E.; Tee, J. J.; Parkin, I. P.; Williams, D. R. Adsorption of volatile organic compounds by industrial porous materials: Impact of relative humidity. *Microporous Mesoporous Mater.* **2020**, *298*, 110090.

(12) Yin, T.; Meng, X.; Jin, L.; Yang, C.; Liu, N.; Shi, L. Prepared hydrophobic Y zeolite for adsorbing toluene in humid environment. *Microporous and Mesoporous Materials* **2020**, *305*, 110327.

(13) Gregis, G.; Schaefer, S.; Sanchez, J.-B.; Fierro, V.; Berger, F.; Bezverkhyy, I.; Weber, G.; Bellat, J.-P.; Celzard, A. Characterization of materials toward toluene traces detection for air quality monitoring and lung cancer diagnosis. *Mater. Chem. Phys.* **2017**, *192*, 374–382.

(14) Fitch, A. N.; Jobic, H.; Renouprez, A. Localization of benzene in sodium-Y-zeolite by powder neutron diffraction. *The Journal of Physical Chemistry* **1986**, *90*, 1311–1318.

(15) Demontis, P.; Yashonath, S.; Klein, M. L. Localization and mobility of benzene in sodium-Y zeolite by molecular dynamics calculations. *The Journal of Physical Chemistry* **1989**, *93*, 5016–5019.

(16) Kitagawa, T.; Tsunekawa, T.; Iwayama, K. Monte Carlo simulations on adsorptions of benzene and xylenes in sodium-Y zeolites. *Microporous Materials* **1996**, *7*, 227–233.

(17) Gonçalves, J. A. S.; Portsmouth, R. L.; Alexander, P.; Gladden, L. F. Intercage and Intracage Transport of Aromatics in Zeolites NaY, HY, and USY Studied by 2H NMR. *The Journal of Physical Chemistry* **1995**, *99*, 3317–3325.

(18) Auerbach, S. M.; Bull, L. M.; Henson, N. J.; Metiu, H. I.; Cheetham, A. K. Behavior of Benzene in Na-X and Na-Y Zeolites: Comparative Study by 2H NMR and Molecular Mechanics. *The Journal of Physical Chemistry* **1996**, *100*, 5923–5930.

(19) Jobic, H.; Fitch, A. N.; Combet, J. Diffusion of Benzene in NaX and NaY Zeolites Studied by Quasi-Elastic Neutron Scattering. *The Journal of Physical Chemistry B* **2000**, *104*, 8491–8497.

(20) Uytterhoeven, L.; Dompas, D.; Mortier, W. J. Theoretical investigations on the interaction of benzene with faujasite. *J. Chem. Soc., Faraday Trans.* **1992**, *88*, 2753–2760.

(21) Hessou, E. P.; Bédé, L. A.; Jabraoui, H.; Semmeq, A.; Badawi, M.; Valtchev, V. Adsorption of Toluene and Water over Cationic-Exchanged Y Zeolites: A DFT Exploration. *Molecules* **2021**, *26*.

(22) Zeng, Y.; Ju, S.; Xing, W.; Chen, C. Computer Simulation of Benzene Adsorbed in All-Silica Y and NaY Zeolites. *Industrial & Engineering Chemistry Research* **2007**, *46*, 242–248.

(23) Daems, I.; Leflaive, P.; Méthivier, A.; Baron, G. V.; Denayer, J. F. Influence of Si:Al-

ratio of faujasites on the adsorption of alkanes, alkenes and aromatics. *Microporous and Mesoporous Materials* **2006**, *96*, 149–156.

(24) Barthomeuf, D.; Ha, B.-H. Adsorption of benzene and cyclohexane on faujasite-type zeolites. Part 2.-Adsorption site efficiency and zeolite field influence at high coverage. *J. Chem. Soc., Faraday Trans. 1* **1973**, *69*, 2158–2165.

(25) González-Galán, C.; Luna-Triguero, A.; Vicent-Luna, J.; Zaderenko, A.; Sławek, A.; de Armas, R. S.; Calero, S. Exploiting the π-bonding for the separation of benzene and cyclohexane in zeolites. *Chemical Engineering Journal* **2020**, *398*, 125678.

(26) Buttefey, S.; Boutin, A.; Mellot-Draznieks, C.; Fuchs, A. H. A Simple Model for Predicting the Na+ Distribution in Anhydrous NaY and NaX Zeolites. *The Journal of Physical Chemistry B* **2001**, *105*, 9569–9575.

(27) Di Lella, A.; Desbiens, N.; Boutin, A.; Demachy, I.; Ungerer, P.; Bellat, J.-P.; Fuchs, A. H. Molecular simulation studies of water physisorption in zeolites. *Phys. Chem. Chem. Phys.* **2006**, *8*, 5396–5406.

(28) Castillo, J. M.; Silvestre-Albero, J.; Rodriguez-Reinoso, F.; Vlugt, T. J. H.; Calero, S. Water adsorption in hydrophilic zeolites: experiment and simulation. *Phys. Chem. Chem. Phys.* **2013**, *15*, 17374–17382.

(29) Salazar, J.; Lectez, S.; Gauvin, C.; Macaud, M.; Bellat, J.; Weber, G.; Bezverkhyy, I.; Simon, J. Adsorption of hydrogen isotopes in the zeolite NaX: Experiments and simulations. *International Journal of Hydrogen Energy* **2017**, *42*, 13099–13110.

(30) Salazar, J. M.; Badawi, M.; Radola, B.; Macaud, M.; Simon, J. M. Quantum Effects on the Diffusivity of Hydrogen Isotopes in Zeolites. *The Journal of Physical Chemistry C* **2019**, *123*, 23455–23463.

(31) Wick, C. D.; Siepmann, J.; Klotz, W. L.; Schure, M. R. Temperature effects on the retention of n-alkanes and arenes in helium-squalane gas-liquid chromatography: Experiment and molecular simulation. *Journal of Chromatography A* **2002**, *954*, 181–190.

(32) Luan, B.; Ferreira, R.; Giro, R.; Elengikal, T.; Gupta, A.; de Oliveira, F.; Liu, S.; Steiner, M.; Peters, T.; Farmahini, A.; Manning, J.; Cleeton, C.; Siperstein, F.; Sarkisov, L.; O Conchuir, B. The role of partial charges in data-driven analytics of gas adsorption simulations. APS March Meeting Abstracts. 2022; p K01.005.

(33) Hogan, A.; Space, B. Next-Generation Accurate, Transferable, and Polarizable Potentials for Material Simulations. *Journal of Chemical Theory and Computation* **2020**, *16*, 7632–7644.

(34) Calero, S.; Dubbeldam, D.; Krishna, R.; Smit, B.; Vlugt, T. J. H.; Denayer, J. F. M.; Martens, J. A.; Maesen, T. L. M. Understanding the Role of Sodium during Adsorption: A Force Field for Alkanes in Sodium-Exchanged Faujasites. *Journal of the American Chemical Society* **2004**, *126*, 11377–11386.

(35) García-Sánchez, A.; Ania, C. O.; Parra, J. B.; Dubbeldam, D.; Vlugt, T. J. H.; Krishna, R.; Calero, S. Transferable Force Field for Carbon Dioxide Adsorption in Zeolites. *The Journal of Physical Chemistry C* **2009**, *113*, 8814–8820.

(36) Martin-Calvo, A.; Gutiérrez-Sevillano, J. J.; Parra, J. B.; Ania, C. O.; Calero, S. Transferable force fields for adsorption of small gases in zeolites. *Phys. Chem. Chem. Phys.* **2015**, *17*, 24048–24055.

(37) Dubbeldam, D.; Calero, S.; Vlugt, T. J. H.; Krishna, R.; Maesen, T. L. M.; Smit, B. United Atom Force Field for Alkanes in Nanoporous Materials. *The Journal of Physical Chemistry B* **2004**, *108*, 12301–12313.

(38) Schuler, L. D.; Van Gunsteren, W. F. On the choice of dihedral angle potential energy functions for n-alkanes. *Molecular Simulation* **2000**, *25*, 301–319.

(39) Schuler, L. D.; Daura, X.; van Gunsteren, W. F. An improved GROMOS96 force field for aliphatic hydrocarbons in the condensed phase. *Journal of Computational Chemistry* **2001**, *22*, 1205–1218.

(40) da Silva, G. C. Q.; Silva, G. M.; Tavares, F. W.; Fleming, F. P.; Horta, B. A. C. Are all-atom any better than united-atom force fields for the description of liquid properties of alkanes? *Journal of Molecular Modeling* **2020**, *26*.

(41) da Silva, G. C.; Silva, G. M.; Tavares, F. W.; Fleming, F. P.; Horta, B. A. Are all-atom any better than united-atom force fields for the description of liquid properties of alkanes? 2. A systematic study considering different chain lengths. *Journal of Molecular Liquids* **2022**, *354*, 118829.

(42) Romanielo, L. L.; Pereira, M. G. M. V.; Arvelos, S.; Maginn, E. J. Use of a New Size-Weighted Combining Rule to Predict Adsorption in Siliceous Zeolites. *Journal of Chemical & Engineering Data* **2020**, *65*, 1379–1395.

(43) Dang, L. X. Mechanism and Thermodynamics of Ion Selectivity in Aqueous Solutions of 18-Crown-6 Ether: A Molecular Dynamics Study. *Journal of the American Chemical Society* **1995**, *117*, 6954–6960.

(44) Nejahi, Y.; Soroush Barhaghi, M.; Mick, J.; Jackman, B.; Rushaidat, K.; Li, Y.; Schwiebert, L.; Potoff, J. GOMC: GPU Optimized Monte Carlo for the simulation of phase equilibria and physical properties of complex fluids. *SoftwareX* **2019**, *9*, 20–27.

(45) Martin, M. G.; Siepmann, J. I. Novel Configurational-Bias Monte Carlo Method for Branched Molecules. Transferable Potentials for Phase Equilibria. 2. United-Atom Description of Branched Alkanes. *The Journal of Physical Chemistry B* **1999**, *103*, 4508–4517.

(46) Cummings, P. T.; McCabe, C.; Iacovella, C. R.; Ledeczi, A.; Jankowski, E.; Jayaraman, A.; Palmer, J. C.; Maginn, E. J.; Glotzer, S. C.; Anderson, J. A.; et al., Open-

source molecular modeling software in chemical engineering focusing on the Molecular Simulation Design Framework. *AIChE Journal* **2021**, *67*, e17206.

(47) Klein, C.; Sallai, J.; Jones, T. J.; Iacovella, C. R.; McCabe, C.; Cummings, P. T. In *Foundations of Molecular Modeling and Simulation: Select Papers from FOMMS 2015*; Snurr, R. Q., Adjiman, C. S., Kofke, D. A., Eds.; Molecular Modeling and Simulation; Springer Singapore, 2016; pp 79–92.

(48) Klein, C.; Summers, A. Z.; Thompson, M. W.; Gilmer, J. B.; McCabe, C.; Cummings, P. T.; Sallai, J.; Iacovella, C. R. Formalizing atom-typing and the dissemination of force fields with foyer. *Computational Materials Science* **2019**, *167*, 215–227.

(49) Humphrey, W.; Dalke, A.; Schulten, K. VMD – Visual Molecular Dynamics. *Journal of Molecular Graphics* **1996**, *14*, 33–38.

(50) Vlugt, T. J. H.; García-Pérez, E.; Dubbeldam, D.; Ban, S.; Calero, S. Computing the Heat of Adsorption using Molecular Simulations: The Effect of Strong Coulombic Interactions. *Journal of Chemical Theory and Computation* **2008**, *4*, 1107–1118.

(51) Pujol, Q.; Weber, G.; Bellat, J.-P.; Grätz, S.; Krusenbaum, A.; Borchardt, L.; Bezverkhyy, I. Potential of novel porous materials for capture of toluene traces in air under humid conditions. *Microporous and Mesoporous Materials* **2022**, 112204.

(52) Zheng, H.; Zhao, L.; Ji, J.; Gao, J.; Xu, C.; Luck, F. Unraveling the Adsorption Mechanism of Mono- and Diaromatics in Faujasite Zeolite. *ACS Applied Materials & Interfaces* **2015**, *7*, 10190–10200.

(53) Benoit, F. Adsorption des mercaptans légers sur des zéolithes. Ph.D. thesis, Université de Bourgogne, 2007.

(54) Pilverdier, E. Apport de la calorimeétrie à la connaissance des interactions zéolithe-

adsorbat et corrélations avec les données structurales. Ph.D. thesis, Université de Bourgogne, 1995.

(55) Marshall, M. S.; Steele, R. P.; Thanthiriwatte, K. S.; Sherrill, C. D. Potential Energy Curves for Cation-π Interactions: Off-Axis Configurations Are Also Attractive. *The Journal of Physical Chemistry A* **2009**, *113*, 13628–13632.

(56) Vitale, G.; Mellot, C. F.; Bull, L. M.; Cheetham, A. K. Neutron Diffraction and Computational Study of Zeolite NaX: Influence of SIII' Cations on Its Complex with Benzene. *The Journal of Physical Chemistry B* **1997**, *101*, 4559–4564.

(57) Zheng, H.; Zhao, L.; Yang, Q.; Dang, S.; Wang, Y.; Gao, J.; Xu, C. Insight into the adsorption mechanism of benzene in HY zeolites: the effect of loading. *RSC Adv.* **2016**, *6*, 34175–34187.

TOC Graphic